

Spin-polarized surface states close to adatoms on Cu(111)

B. Lazarovits¹, L. Szunyogh^{1,2}, P. Weinberger¹¹Center for Computational Materials Science,
Technical University Vienna,
A-1060, Gumpendorferstr. 1a., Vienna, Austria²Department of Theoretical Physics and
Center for Applied Mathematics and Computational Physics,
Budapest University of Technology and Economics,
Budafoki út 8., H-1521 Budapest, Hungary
(Dated: April 14, 2024)

We present a theoretical study of surface states close to 3d transition metal adatoms (Cr, Mn, Fe, Co, Ni and Cu) on a Cu(111) surface in terms of an embedding technique using the fully relativistic Korringa-Kohn-Rostoker method. For each of the adatoms we found resonances in the s -like states to be attributed to a localization of the surface states in the presence of an impurity. We studied the change of the s -like densities of states in the vicinity of the surface state band-edge due to scattering effects mediated via the adatom's d -orbitals. The obtained results show that a magnetic impurity causes spin-polarization of the surface states. In particular, the long-range oscillations of the spin-polarized s -like density of states around an Fe adatom are demonstrated.

PACS numbers: 73.20.At, 73.20.Hb, 73.22.-f

INTRODUCTION

Following the first experimental observation of a surface band at Cu(111) in terms of angle-resolved photoemission (ARPES) [1] electrons at closed packed surfaces of noble metals have been at the center of much experimental [2, 3, 4, 5, 6, 7] and theoretical [8, 9, 10] attention. For a pristine surface the energies of Shockley surface states lie in the 'gap' around the L-point of the bulk Brillouin Zone, their wavefunctions being confined to the surface. The corresponding dispersion relations have been determined by ARPES and were found to be two-dimensional free-electron like parabolas [1, 2, 6]. One of the highly interesting features of this phenomenon is the response to perturbations caused by placing, e.g., adatoms on the surface. As to be expected such a response is characterized by long range Friedel-like charge oscillations governed by the dispersion relation of the two-dimensional surface electron gas. The existence of long range interactions between adatoms on surfaces supporting surface states can lead to the formation of an atomic superlattice as recently shown both experimentally [7] and theoretically [10]. Until recently STM studies of atoms on well defined Cu, Ag and Au(111) surfaces imaged only the charge distribution of the surface electrons [3, 4, 5]. Remarkable developments in spin polarized STM [11], however, are expected to detect spatial variations in the magnetic density, which in turn might provide an understanding of the magnetic behavior of this kind of systems [12, 13, 14, 15]. Evidently, this also opens up the possibility of designing magnetic nanostructures for both scientific and technological purposes.

In accordance with a theoretical prediction by Borisov et al. [16], by using STM at 7 K, Limot et al. [17] very recently reported on an adatom-induced localization

of the surface states electrons on Cu(111) and Ag(111) surfaces. The existence of such resonances for a single Cu adatom was also shown theoretically by Olsson et al. [18] in terms of a parameter-free pseudopotential method. The appearance of a peak in the density of states (DOS) just below the surface state band can be attributed to a theorem by Simon claiming the existence of a bound state for any attractive potential in two dimensions [18, 19]. It was demonstrated in Ref. [17] by comparing results for Co and Cu adatoms on Cu(111) that the type of adsorbate influences the shape of the adatom-induced resonance. For this very reason we performed a systematic study for a series of 3d impurities (Cr, Mn, Fe, Co, Ni and Cu) on Cu(111) in order to identify spin-dependent features of the occurring resonance.

METHOD OF CALCULATIONS

Within multiple scattering theory the electronic structure of an ensemble of non-overlapping potentials is described by the so-called scattering path operator (SPO) matrix (for more details see, e.g., Ref. [20]). The SPO matrix c that refers to a finite cluster C embedded into a host system can be obtained from the following Dyson equation [21],

$$c(E) = h(E) I - (t_h^{-1}(E) - t_c^{-1}(E)) h(E)^{-1}; \quad (1)$$

where $t_h(E)$ and $h(E)$ denote the single-site scattering matrix and the SPO matrix for the unperturbed host confined to sites in C , respectively, while t_c denotes the single-site scattering matrices of the embedded atom s . Note, that Eq. (1) takes into account all scattering events both inside and outside the cluster.

First, a fully self-consistent (SC) calculation is performed for the Cu (111) surface by means of the screened Korringa-Kohn-Rostoker (SKKR) method [22]. Then for single adatom placed on top of Cu (111) the multiple scattering problem is solved self-consistently in terms of the embedding method discussed in details in Ref. [21]. The self-consistent calculations for both the semi-infinite Cu (111) host and the adatom were performed using the atomic sphere approximation (ASA) and the local spin-density approximation in the parameterization of Vosko et al. [23]. Due to the fully relativistic treatment applied the orientation of the effective magnetic field had to be specified: it was chosen to point along the z axis (normal to the surface). In order to evaluate the inevitable Brillouin-zone integrations, in the self-consistent calculations $70 k_k$ points were used in the irreducible wedge of the surface Brillouin-zone (SBZ). For the calculation of the t -matrices and for the multipole expansion of the charge densities, necessary to evaluate the Madelung potentials, a cutoff of $\ell_{\max} = 2$ was assumed. Energy integrations were performed by sampling 16 points on a semicircular contour in the complex energy plane according to an asymmetric Gaussian quadrature. The densities of states were calculated parallel to the real energy axis with an imaginary part of 5 mRyd by sampling about 2200 k_k points within the irreducible wedge of the SBZ. In the present calculations no attempt was made to include surface relaxations: the geometry was taken to be identical to an ideal Cu bulk fcc lattice (lattice constant $a_0 = 3.614 \text{ \AA}$).

RESULTS AND DISCUSSION

In order to determine the dispersion relation and the effective mass of the surface electrons Bloch-spectral functions (BSF) [24] were evaluated in terms of the SKKR method for k -points between the Γ and K points in the fcc(111) SBZ close to the Fermi energy. It should be recalled that the dispersion relation of the surface state band can be defined by the position of the maxima in the BSF. In agreement with experiments the calculated dispersion relation is a free-electron like parabola as indicated in Fig. 1. The bottom of the calculated surface state band is only about 0.3 eV below the Fermi energy which is a bit smaller than the experimental values (0.4 eV) [2, 6]. Also in good agreement with the experimental data [2] is the corresponding effective mass $m^* = 0.37 m_e$ as obtained using an appropriate fitting procedure. In Fig. 1 also the density of the surface states in the vicinity of the band-edge is displayed. Shown is the s -like DOS of the first vacuum (empty sphere) layer as integrated over a sphere of a radius of $0.15/a.u.$ centered around Γ of the SBZ. Note that the corresponding DOS at the substrate layers decays exponentially with increasing distance from the surface. As our calculations

do not include structural defects (e.g., steps) at the surface, electron-electron interaction beyond the density functional theory or electron-phonon interaction, the rather broad onset of the surface-state band is a direct consequence of using an imaginary part of 5 mRyd for the energy when calculating the DOS, see the solid line on the right of Fig. 1. In order to justify this argument, only for this particular case, we also performed calculations with imaginary parts of 2, 1 and 0.5 mRyd displayed in Fig. 1 in terms of dash-dotted, dashed and dotted lines, respectively. As can be seen, by decreasing the imaginary part of the energy the onset of the surface-band approaches a step-like behavior. The experimental onset ($\sim 30 \text{ meV}$ [17]) is fairly well recovered in case of 1 mRyd for the imaginary part. It should be noted that, in order to smooth out spurious oscillations in the calculated density of the surface states, in this case a sampling of more than 50 000 k_k points within the irreducible wedge of the SBZ (about 2000 k_k points for $|k_k| < 0.15$) was needed, see also a recent theoretical STM study of Hoffer and Garcia-Lekue [25]. Fortunately, however, applying a Lorentzian broadening of 5 mRyd ($\sim 70 \text{ meV}$) for the DOS turned out to be sufficient to resolve the adatom induced surface states to be studied in this paper.

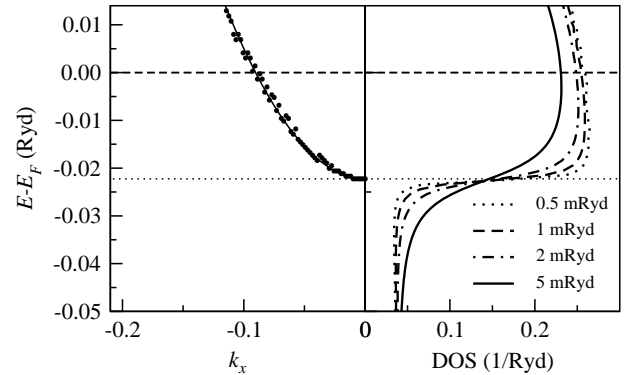


FIG. 1: Left panel: Positions of maxima in the Bloch spectral functions near to the Γ point of the SBZ (dots). The solid line refers to a parabolic fit. It should be noted that only the first third of the SBZ is displayed ($|k| \leq 0.65$). Right panel: Density of the surface states ($|k_k| < 0.15$) close to a clean Cu (111) surface. The different values for the imaginary part of the energy used are displayed explicitly. The Fermi energy and the bottom of the surface state band are indicated by a dashed and a dotted horizontal lines, respectively.

In Fig. 2 the calculated s -DOS and total DOS (insets) for the chosen series of adatoms are presented as projections with respect to the two spin directions. As is also evident from the spin-split peaks in the total DOS, dominated mainly by d -like contributions, the Cr, Mn, Fe, Co and Ni adatoms on Cu (111) were found to be magnetic with spin moments of $S_{Cr}^z = 4.21 \mu_B$, $S_{Mn}^z = 4.39 \mu_B$, $S_{Fe}^z = 3.27 \mu_B$, $S_{Co}^z = 2.02 \mu_B$ and $S_{Ni}^z = 0.51 \mu_B$, while the Cu adatom is non-magnetic. It should be noted that

within a relativistic description the electronic spin is not a constant of motion. In the present cases, however, characterized by large exchange splittings and weak spin-orbit interactions it is quite illustrative to view the two spin channels separately by making use of the approximation discussed in Ref. [26].

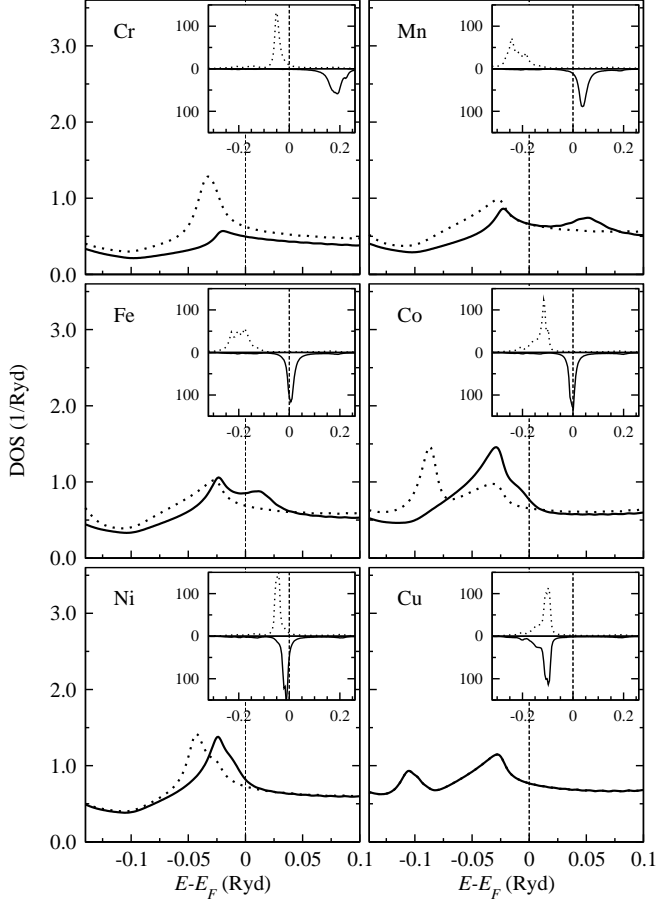


FIG. 2: Calculated spin-projected s-like density of states at the impurity positions. Insets: Spin-projected total density of states of the adatoms. In each entry, the majority and the minority spin DOS's are depicted by dotted and solid lines, respectively.

Concentrating first on the case of the Cu adatom, quite a broad peak is found just below the bottom of the surface state band ($E = 0.025$ Ryd). The appearance of this peak indicates that adatoms act as an effective attractive potential for surface state electrons inducing thus a certain degree of localization. The widths and positions with respect to the surface state band edge of the adatom-induced peak agrees well with the one obtained in Ref. [18]. The calculated resonance width being also in agreement with Ref. [18] is, however, approximately three times larger than experimentally measured [17]. This disagreement with the experiment can most probably be attributed again to the rather large Lorentzian broadening of the calculated DOS.

The fairly narrow d-band of the Cu adatom lies well below the 2D surface band ($E_d = 0.1$ Ryd). It can therefore be assumed that the adatom-induced resonance at $E = 0.025$ Ryd is hardly influenced by d-like states. This allows us to consider the Cu adatom as a reference when identifying effects of d-states on the adatom-induced resonance in the case of other impurities. In line with Ref. [18], a peak in the s(DOS of the Cu adatom can be observed just at the peak position of the d-band. This is a direct consequence of the hybridization between s and d type atomic orbitals as illustrated in Fig. 3 using group theoretical arguments. It is important to note that in order to make use of a well-defined non-relativistic classification of the densities of states in terms of symmetry adapted spherical harmonics, only in this case we "switched off" the spin-orbit coupling by applying the so-called scaling scheme proposed by Ebert et al. [27]. In the upper panel of this figure the d(DOS is decomposed into three components: two of them corresponding to the two-dimensional irreducible representation (E) of the C_{3v} point group, namely, according to the following sets of symmetrized basis functions $fd_{xy}; d_{x^2-y^2}g$ and $fd_{xz}; d_{yz}g$, and one to a one-dimensional representation (A_1), namely, with respect to $fd_{z^2}g$. Clearly enough, the s-states that correspond to A_1 symmetry can hybridize only with d_{z^2} states as is apparent from the line-shapes of the corresponding DOS's in Fig. 3.

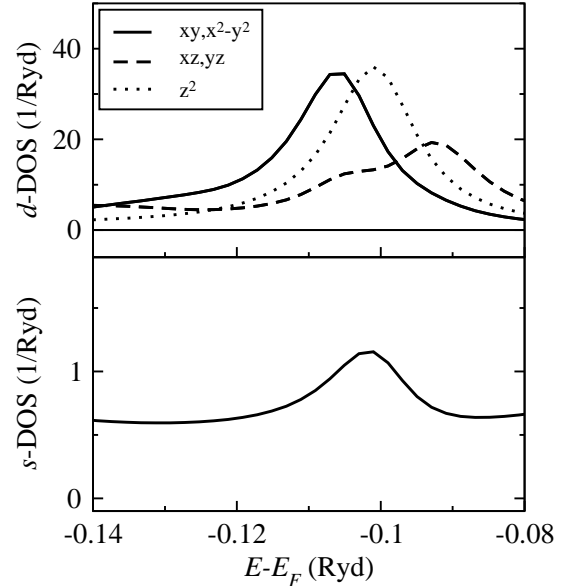


FIG. 3: Upper panel: Calculated d(DOS of a single Cu impurity on a Cu(111) surface as partitioned into d_{xz} , d_{yz} , d_{xy} , d_{z^2} and $d_{x^2-y^2}$ like contributions. Lower panel: s(DOS at the same site. The DOS's presented in this figure correspond to one of the spin projections.

From Fig. 2 the appearance of the adatom-induced localized state is also obvious in the case of the magnetic impurities as only a slight variation of its position in en-

ergy occurs. This indicates that each kind of impurity acts in a similar manner as an attractive potential well for the 2D electron gas. As can be seen, however, in the case of magnetic adatoms the shape of the adatom-induced resonance is different for the two spin projections. This observation can be well explained in terms of the energetic position of the corresponding d-bands of the impurities. For Mn, Fe and also for Co the majority d-band lies reasonably deep below the adatom-induced resonance. Therefore, the line shape of one (say majority) spin-projected sDOS around $E = 0.025$ Ryd is practically unchanged as compared to the Cu case. Within the energy range displayed, an s-d hybridized peak in the majority sDOS is seen for Co around -0.09 Ryd. An analysis in terms of symmetry-adapted spherical harmonics (basis functions) as discussed in the case of the Cu adatom applies also in this case. For Cr and Ni the position of the majority d-band is just at the bottom of surface band. The adatom-induced resonance appears therefore for Ni just as a small shoulder on the upper side of the s-d hybridized peak, while for Cr the resonance can hardly be traced at all.

For all magnetic adatoms investigated the minority d-band overlaps with the 2D surface state band. In the series Cr to Ni its position moves downwards in energy, its width decreases monotonously. For Mn and Fe a moderately well-developed peak can be seen at the position of the very sharp d-band, while for Co and Ni just a small 'hump' in the minority sDOS is visible. The occurrence of these structures is of similar origin as the s-d hybridized peaks in the majority spin channel: the continuum-states experience resonant scattering due to an overlap with an adatom's d orbitals giving thus rise to well-known virtual bound state resonances. As can be shown in terms of a non-interacting Anderson model, this effect is proportional to the DOS of the continuum band, which decreases if the position of the d-band moves towards the bottom of the surface band. This explains qualitatively the trend for the width of the minority d-band. It is, however, apparent that the minority spin adatom-induced resonance peak ($E = 0.025$ Ryd) is considerably larger for Co and Ni as for Cu, a fact which might be attributed to a strengthening of the localization of the 2D surface electrons due to d-like virtual bound states very close in energy.

In Fig. 4 the sDOS for both spin directions is shown for a site at selected distances measured with respect to an Fe adatom in the same plane (parallel to the surface). It can be observed that the line shapes related to the adatom-induced resonance and the minority spin resonant scattering vanish in fact at a radius of about two in units of the 2D (in plane) lattice constant. Beyond this radius a lineshape characteristic for the 2D surface-state band appears to evolve, however, with a broader onset than for the pristine Cu(111) surface. This broadening can again be attributed to the interaction (overlap) be-

tween the surface states and the d-states of an adatom.

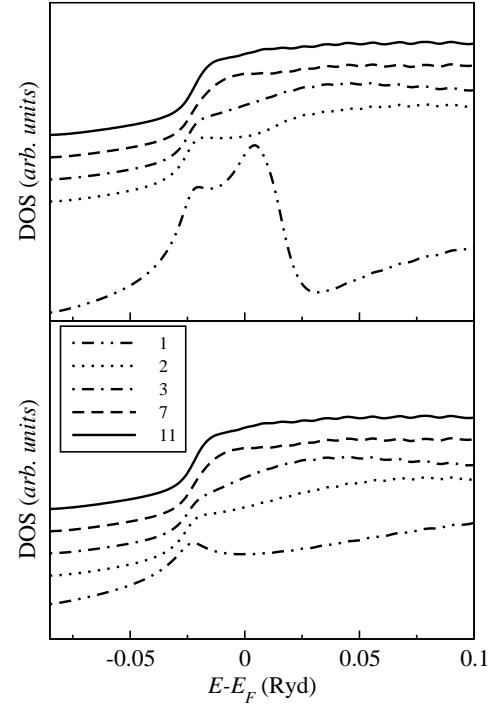


FIG. 4: Calculated minority spin (upper panel) and majority spin (lower panel) sDOS's at a site in the same plane as a single Fe impurity on a Cu(111) surface with respect to the distance between these two sites. The distance (in units of the two-dimensional lattice constant) is indicated in the legend of the lower panel.

At a distance of seven 2D lattice constants (17.9 \AA) the sDOS is practically the same as calculated for the clean Cu(111) surface. A long-ranged oscillatory behavior of the densities of states can, however, still be resolved. In Fig. 5 the DOS at a selected energy, namely, 34 mRyd above the bottom of the surface-state band is displayed for both spin channels as a function of the distance from an Fe adatom. A simple estimate of the wavelength of the 2D Friedel oscillation,

$$\sim \frac{\pi}{2m E} ; \quad (2)$$

gives $15 \text{ \AA} \approx 6 a_{2D}$ that can be read off from Fig. 5. As shown in the inset of Fig. 5, a magnetic impurity also induces long-range oscillations in the magnetization density of states (M DOS, defined as the difference of the spin-projected DOS's), with the same period. Clearly, these oscillations in the M DOS lead to a long-range RKKY interaction on noble metal (111) surfaces as discussed, e.g., in Ref. [10].

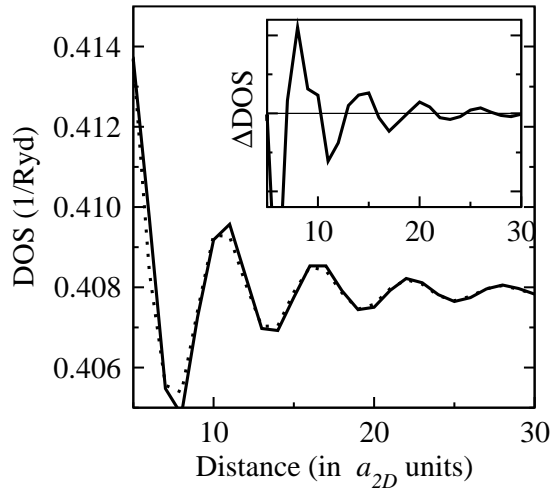


FIG. 5: Calculated minority spin (solid line) and majority spin (dotted line) DOS's at $E_F = 0.012$ Ryd of a site positioned in the same plane but at a certain distance from a single Fe impurity on a Cu(111) surface. Inset: difference of the spin projected DOS's.

CONCLUSION

We presented a series of calculations for spin-dependent surface states close to 3d transition metal adatoms (Cr, Mn, Fe, Co, Ni and Cu) on a Cu(111) surface. In agreement with previous theoretical [18] and experimental [17] studies the appearance of an adatom-induced resonance just below the surface state band edge is shown. The occurrence of an additional peak in the DOS caused by the adatom's d_{z^2} -states was found below the adatom-induced resonance not only for a Cu adatom [18] but also for magnetic adatoms in the majority spin channel. We also found evidence of an interaction of the minority spin d-states of the magnetic impurities and the surface state continuum, that for Co and Ni possibly explains the remarkable enhancement of the adatom-induced resonance peak in the minority spin channel. The different shape of the adatom-induced resonance for Cu and Co was indeed observed in experiments [17] and is in qualitative agreement with our calculations. Finally, we pointed out the existence of long-range spin-polarized oscillations of the surface states around a magnetic impurity being the very origin of a 2D RKKY interaction.

Financial support was provided by the Center for Computational Materials Science (Contract No. GZ 45.531, GZ 98.366), the Austrian Science Foundation (Contract No. W 004), the Hungarian Research and Technological Innovation Council and the Bundesministerium für Auswertige Angelegenheiten of Austria (Contract No. A-

3/03) and the Hungarian National Scientific Research Foundation (OTKA T 037856 and T 046267).

- [1] P. O. Gartland and B. J. Slagsvold, Phys. Rev. B 12, 4047 (1975).
- [2] S. D. Kevan, Phys. Rev. Lett. 50, 526 (1983).
- [3] M. F. Crommie, C. P. Lutz, D. M. Eigler, and E. J. Heller, Physica D 83, 98 (1995).
- [4] M. F. Crommie, C. P. Lutz, D. M. Eigler, and E. J. Heller, Surface Science 361/362, 864 (1996).
- [5] H. C. Manoharan, C. P. Lutz, and D. M. Eigler, Nature 403, 512 (2000).
- [6] F. Baumberger, T. Greber, and J. Osterwalder, Phys. Rev. B 64, 195411 (2001).
- [7] F. Silly, M. Pivetta, M. Temes, F. Patthey, J. P. Pelz, and W. D. Schneider, Phys. Rev. Lett. 92, 016101 (2004).
- [8] G. Horn and J. B. Pendry, Phys. Rev. B 50, 18607 (1994).
- [9] J. Li, W. D. Schneider, R. Berndt, O. R. Bryant, and S. Crampin, Phys. Rev. Lett. 81, 4464 (1998).
- [10] V. S. Stepanyuk, L. Niebergall, R. C. Longo, W. Hergert, and P. Bruno, Phys. Rev. B 70, 075414 (2004).
- [11] M. Bode, Rep. Prog. Phys. 65, 523 (2003).
- [12] K. Hallberg, A. A. Correa, and C. A. Balseiro, Phys. Rev. Lett. 88, 066802 (2002).
- [13] A. A. Correa, F. A. Reboredo, and C. A. Balseiro, Phys. Rev. B 71, 035418 (2005).
- [14] B. Lazarovits, B. Ujfalussy, L. Szunyogh, B. L. Gyor'y, P. Weinberger, J. Phys.: Condens. Matter 17, S1037 (2005).
- [15] V. S. Stepanyuk, L. Niebergall, W. Hergert, and P. Bruno, Phys. Rev. Lett. 94, 187201 (2005).
- [16] A. G. Borisov, A. K. Kazansky, and J. P. Gauyacq, Phys. Rev. B 65, 205414 (2002).
- [17] L. Linot, E. Pehlke, J. Kroger, and R. Berndt, Phys. Rev. Lett. 94, 036805 (2005).
- [18] F. E. Olsson, M. Persson, A. G. Borisov, J. P. Gauyacq, J. Lagoutei, and S. Folsch, Phys. Rev. Lett. 93, 206803 (2004).
- [19] B. Simon, Ann. Phys. (N.Y.) 97, 279 (1976).
- [20] J. Zabloudil, R. Hammerling, L. Szunyogh, and P. Weinberger, Electron Scattering in Solid Matter (Springer-Verlag, Berlin Heidelberg, 2005).
- [21] B. Lazarovits, L. Szunyogh, and P. Weinberger, Phys. Rev. B 65, 104441 (2002).
- [22] L. Szunyogh, B. Ujfalussy, and P. Weinberger, Phys. Rev. B 51, 9552 (1995).
- [23] S. H. Vosko, L. W.ilk, and M. Nusair, Can. J. Phys. 58, 1200 (1980).
- [24] J. S. Faulkner and G. M. Stocks, Phys. Rev. B 21, 3222 (1980).
- [25] W. A. Hofer and A. Garcia-Lekue, Phys. Rev. B 71, 085401 (2005).
- [26] J. B. Staunton, B. L. Gyor'y, J. Poulter, and P. Strange, J. Phys. C 21, 1595 (1988).
- [27] H. Ebert, H. Freyer, A. Vemes, and G. Guo, Phys. Rev. B 53, 7721 (1996).